Growth of PbSe quantum-dots within high-index lead-phosphate glass for infrared saturable absorbers

Pradeesh Kannan*, Amol Choudhary, Benjamin Mills, Xian Feng and David P.Shepherd

Optoelectronics Research Centre, University of Southampton,

Southampton, SO17 1BJ, United Kingdom

Abstract: PbSe quantum dots (QDs) were grown in high-refractive-index low-melting-temperature lead-phosphate glass. The lowest energy exciton transition of the QDs was tuned over a wide range within the infrared spectral region (0.93 μm to 2.75 μm) by a controlled heat treatment. The measured QD radius ranged between 2 nm and 5.3 nm, with a time (*t)* dependence of $t^{0.29}$ for long dwelling times during the heat treatment, indicating that the QD growth mechanism tends to follow Lifshitz-Slyozov-Wagner theory. The QD saturable absorber behaviour at 1.2 μm had a measured saturation fluence of ~2.1 μJ/cm^2.

I. Introduction

Semiconductor quantum dots (QDs) are of interest for optoelectronics since they demonstrate active properties allowing modulation of light, optical nonlinearity, optical gain, and lasing.[1-4] These properties are observed at wavelengths close to the quantum optical transitions in the QDs. The dependence of the transition energy on QD size allows tuning of these effects to the wavelength of a specific light source, and resonance tuning is possible if the QDs have a narrow size-distribution. QDs of IV–VI materials such as PbS and PbSe offer access to the regime of strong quantum confinement due to their relatively large exciton Bohr radii. The electron and hole masses are almost identical in the bulk, so the electron and hole wave

* Corresponding author, Email: pk2e10@orc.soton.ac.uk, Ph: +44 (0) 23 8059 9254, Fax: +44 (0) 23 8059 3142

functions will be similar, approximating an ideal quantum dot in the strong-confinement limit. For PbSe, the exciton Bohr radii is ~ 46 nm, which is much larger than in any other semiconductors. These large radii allow strong confinement to be achieved in relatively large nanostructures, providing a wide tuneability of the first exciton transition energy.

Growing QDs in glasses offers attractive applications such as saturable absorbers for passive Q-switching and mode-locking in solid-state lasers[1-3] and active media for lasers[4], in a robust all solid-state format. Present research work on integrated photonics[5,6] provides a motivation for the fabrication of QD-containing glasses with a wide range of refractive indices so as to have proper index matching for reduced reflection losses and/or as part of a guided-wave index structure. In this work we developed a high-index low-melting-temperature glass containing narrowly distributed PbSe QDs. Through controlled heat treatment, the exciton peak of the QD was readily tuned between 0.93 μm and 2.75 μm.

Doping oxide glasses with high semiconductor concentration encourages the nucleation and growth of QDs and also results in a high yield of QDs. The limiting issues are low solubility of semiconductors in oxide glass melts and volatility of the semiconductors due to oxidation and/or evaporation during the glass melting process. While the boiling points of PbSe and PbS are ~ 1100 ^{o}C, the melting temperature of silicate and borosilicate glasses are usually ~1400 to 1600 °C. [7-10] The reported refractive indices of QD grown in silicate, borosilicate and phosphate glasses are below 1.55.[7-10] Though, there are reports on growing QDs in high-index lead-silicate glass,[11] the melting point (~1400^{o}C) of lead-silicate glass is much higher than the boiling point of PbSe/PbS semiconductors (~1100^{o}C), which results in loss of semiconductor due to evaporation. Thus glasses with low melting temperature such as phosphor-tellurite and lead-phosphate are preferable to reduce the loss due to evaporation, thereby maintaining high semiconductor concentration in the final glass matrix. These glass compositions also provide a wide range of tuneability of the host refractive indices to match

the index of a specific laser crystal. Lead-phosphate ($PbO-P_2O_5$) glass,[12] in particular, should offer the additional advantage of including higher concentrations of PbSe by substitution of the PbO already within the glass, while at the same time maintaining a constant mol.% of lead and other glass components and hence limits the change in refractive index due to PbSe doping once a desired refractive index has been achieved.

II. Experimental Details

Glass batches of 20 g of (50-x) PbO - 10ZnO - $40P_2O_5$ - xPbSe (named here as PZPx) (x=0, 2, 6, 10 mol%) were prepared by a standard melting-quenching approach in a dry atmosphere. The glasses were melted at 900^{o}C for 3hrs and casted onto a brass mould and subsequently annealed at 350^{o}C to release the strain. QDs were grown in PZP10 glass by heat treating the sliced glasses between 370^{o}C and 400^{o}C with dwelling time varying from 2hrs to 24hrs. Absorption spectra of heat treated and polished glasses were recorded using a Cary Varian 500 spectrometer and thermal analysis was carried out using a Perkin Elmer Thermo Gravimetry/Differential Thermal Analyser (TG/DTA). The refractive indices were measured with a white light ellipsometer over the range 300nm-1600nm. Energy dispersive X-ray analysis (EDX) was carried out with a Zeiss Evo50 scanning electron microscope (SEM) fitted with INCA 250 x-ray analysis system and transmission electron microscope (TEM) images were recorded with a Jeol 3010.

III. Results and Discussion

On increasing the PbSe concentration, the Urbach absorption edge of the PZPx glass, before growth of QDs, showed a red shift (Fig. 1a). The corresponding optical band gaps (E_{gg}) were estimated from the absorption coefficient (α) data and the relation[13] $\alpha hv=B(hv-E_{gg})^2$, where hv is the photon energy in eV and B is the band tailing parameter. Thus the x-intercept of the linear fit to the absorption edge from the plot $(\alpha hv)^{1/2}$ vs hv gives E_{gg} (Fig. 1a). The estimated E_{gg} decreased from 3.6 eV to 2 eV with increasing PbSe. The decrease in E_{gg} and the

corresponding colour change from light yellow to orange and dark red, for PZP2, PZP6 and PZP10 respectively, indicated the enrichment of the Se concentration within the glass.[14] The composition (in weight percentage) of the glasses were identified by EDX. Figure 1b shows the EDX spectrum of the PZP10 glass. From the inset to Fig. 1b it can be seen that the oxygen wt.% decreased with increasing PbSe mol%. Having maintained all the experimental parameters the same for all the fabricated glasses (PZPx), the decrease in oxygen concentration from ~27% (for PZP0) to ~17% (PZP10) could be attributed to an increase in Se concentration.

Figure 2a shows the measured refractive indices of PZP0 and PZP10 glasses over the wavelength range 300 nm to 1600 nm. Though there are variations in refractive index in the visible region, the index variation above 800nm is $< 7 \times 10^{-3}$. The indices of both the glasses are very similar at near infrared wavelengths and thus substituting PbO with PbSe gives the advantage of maintaining a nearly constant refractive index even at high PbSe doping concentrations. DTA measurements were performed for PZP10 glass at scan rate of 10 ^{o}C/min (Fig. 2b). The glass transition temperature (T_g) and crystallisation temperature (T_x) were identified from the DTA curve as ~350 ^{o}C and ~465 ^{o}C respectively.

Quantum dots were grown inside PZP10 glass by heat treatments within the temperature range 370 ^{o}C to 400 ^{o}C (between T_g and T_x) for dwelling times varying between 2 hours (hrs) and 24 hrs. The colour of the glass samples gradually changed from dark red to brown and then to black. The formation of PbSe QDs within the glass matrix was confirmed by TEM. For heat treatment at 370 ^{o}C, QD nucleation and growth was observed for dwelling times above 6hrs. For higher temperatures, e.g. 400 ^{o}C, QD nucleation and growth was observed for dwelling times as short as 30 minutes.

Figure 3a shows the high-resolution TEM image of PZP10 glass heat treated at 380 ^{o}C for 12 hrs. The observed fringe patterns of different planes of QD crystals, whose physical

extent is indicated by the dotted rings, were well resolved at higher magnifications (Fig. 4). The interplanar distances (*d*-spacing) calculated from the Fourier transform of the fringe patterns are d_{111}= 3.53 Å, d_{200}= 3.08 Å and d_{220}= 2.18 Å. One such Fourier transform is shown as the inset of Fig. 4 (of the *220* plane). The calculated *d*-spacings are well-matched to the *d*-spacings of PbSe planes.[15] The distribution of the QD radius was sampled from three TEM images (one of the TEM image is shown in Fig. 3a) and presented in Fig. 3b. The measured QD radius vary between 3.1 nm and 3.5 nm peaking at ~3.3 nm (± 0.2 nm variation in QD radius). The absorption spectrum, which is marked with an arrow in Fig. 5a, shows first exciton transition of 3.3 nm QDs at ~0.73 eV (i.e. 1.7 μm). This transition is blue shifted with respect to the band gap of bulk PbSe (~0.27 eV) by 0.46 eV due to the quantum-confinement effect.[15] This effect can be used to tune the spectral range of the QD exciton transition to the desired laser emitting wavelength. The saturation of the exciton transitions forms the basis of the passive saturable absorbers useful for pulsed laser devices. From the transition energy, QD size can also be estimated from the equation,[16]

$$E_n = E_g + \frac{n^2 h^2}{8R^2}\left(\frac{1}{m_e^*} + \frac{1}{m_h^*}\right) - \frac{1.8e^2}{\varepsilon R} \quad (1)$$

where n is the order of exciton transition, E_n is the exciton transition energy, E_{Sg} is the bulk PbSe semiconductor band gap, *R* is the radius of QD, *h* is Planck's constant, *ε* is the dielectric constant, and m_e^* and m_h^* are the effective masses of electron and hole and *e*-charge of electron respectively. For PbSe, at T=300 K, E_{Sg}=0.27 eV, m_e^*=0.12*m* and m_h^*=0.07*m*, where *m* is the mass of electron.[17] The known refractive indices of bulk PbSe and the glass matrix were used to calculate the dielectric constant, $\varepsilon=(n_{PbSe}/n_{PZP10})^2$. The calculated QD radius, ~ 3.23 nm for the QD containing glass peaked at ~0.73 eV, is in close agreement with the direct measurements from TEM.

A systematic study of QD size (calculated by eqn. 1) versus dwelling time (t) was carried out on glasses heat treated at 380 ^{o}C. (see Fig. 5a,b). With increased dwelling time, the QD exciton peak red shifted, indicating an increase in QD size. QD radius increased from 2 nm (for t = 2 hrs) to 5.3 nm (for t = 24 hrs), see Fig. 5b. There was also a variation in the magnitude of the absorption peak with dwelling time, with a maximum for energies near 0.6 eV (see Fig. 5a). The rise in the magnitude of the absorption indicated an increase in the number of QDs. During the QD growth process, QDs with size above a critical radius (R_c) remain stable within the glass matrix and those with size less than R_c re-dissolve into the glass matrix.[10] Thus, for shorter dwelling times and hence smaller QDs, the QD number density was less and the corresponding absorption was small. As dwelling time increases, the number of QDs with size greater than R_c increases and hence there is an increase in the absorption. For even longer dwelling times the growth process reaches the Ostwald ripening[18] stage, where the larger particles grow at the expense of the smaller particles. Thus for longer dwelling times the QD number density decreases and there is a corresponding decrease in absorption (see Fig. 5a).

Crystal growth in the initial stages was expected to be a diffusion-controlled process, where the radius R, of the QDs grow with time as $R(t) \alpha t^{1/2}$. During the Ostwald ripening stage, the QD growth assumes a $t^{1/3}$ time-dependence according to the classical Lifshitz-Slyozov-Wagner (LSW) theory,[18] where larger crystals grow by atom-by-atom diffusion. The growth curves for the fabricated PbSe QDs display an $R(t) \alpha t^{0.35}$ dependence at early stages of nucleation and growth (below 10 hrs) and $R(t) \alpha t^{0.29}$ at the later stage of crystal growth (above 11 hrs) (Fig. 3b). The growth exponential (0.29) is higher compared to the previously reported value in glass.[10] QD growth, which follows a $t^{1/3}$ dependence, for long dwelling times, will have a corresponding $t^{-2/3}$ time dependence for the first exciton transition energy, given by the relation[19] $E_{ex}=E_{Sg}+At^{-2/3}$ where A is a constant. For our present PbSe QDs, E_{ex}

shows a linear dependence when plotted against $1/(t^{2/3})$ and a y-intercept value estimated to be ~ 0.30 eV, see inset of Fig. 5a. This compares to the known band gap of bulk PbSe of E_{Sg} ~ 0.27 eV. These results indicate that the growth mechanism tend to follow LSW theory.

The QD-containing glasses fabricated by the method described above should be advantageous for optical applications since the exciton transition covers technologically important wavelengths, ranging from as low as 0.93 μm to as high as 2.75 μm, within the near infrared spectral region. Furthermore, growing QDs in high-index glasses could pave the way for integrated photonic devices based on materials with similarly high index. For example, Ti:Sapphire, a material commonly used for bulk ultrafast lasers,[20] has a refractive index of 1.76 at 800 nm, comparable to the present glass system, and several methods of creating waveguides in these materials have been previously reported.[21]

As a demonstration of useful material properties, the saturation fluence (F_{sat}) of one of the QDs peaked near 1.3 μm (indicated by * in Fig. 5a) was evaluated by measuring the intensity dependent transmission. A 1.12-mm-thick QD-containing glass sample was pumped at 1.2 μm by a femtosecond (fs) laser with pulse duration of 150 fs, average power of up to 70 mW, and repetition rate of 1 kHz. The incident energy fluence on the sample was varied using neutral density filters and the transmission was calculated from the ratio of the pulse energy with and without the sample. This has been plotted against the input energy fluence in Fig. 3c. Using a least squares fit[22] (see Fig. 5c) the saturation fluence and the non-saturable absorption coefficient were estimated to be ~2.1 μJ/cm^2 and ~0.85 cm^{-1} respectively. The estimated value of saturation fluence is comparable to a previously reported QD-containing glass used as a saturable absorber for mode-locking at 1.3 μm.[3]

IV. Conclusions

PbSe quantum dots (QDs) were grown in high-index low-melting-temperature lead-phosphate glass. The lowest energy exciton transition of the QDs was tuned over a wide

range within the infrared spectral region (0.93 μm to 2.75 μm) by controlled heat treatment. Measured QD radii range between 2 nm and 5.3 nm and show a $t^{0.29}$ dependence with long dwelling times, indicating that the QD growth mechanism tends to follow LSW theory. Such high-index QD-containing glasses are promising for optical devices such as ultrafast integrated lasers. As an example, the QDs saturable absorption properties were measured at 1.2 μm, giving a saturation fluence of 2.1 μJ/cm^2, showing its promise as a saturable absorber in pulsed laser systems.

Acknowledgements

This research work was supported by the award of Engineering and Physical Sciences Research Council (UK) grant EP/H035745/1. The authors thank Dr. Alexander A. Lagatsky for useful discussions.

References

[1]P. T. Guerreiro, S. Ten, N. F. Borrelli, J. Butty, G. E. Jabbour, and N. Peyghambarian , "PbS Quantum-Dot Doped Glasses as Saturable Absorbers for Mode Locking of a Cr:Forsterite Laser," *Appl. Phys. Lett.*, **71** [12] 1595-1597 (1997).

[2]A. M. Malyarevich, M. S. Gaponenko, K. V. Yumashev, A. A. Lagatsky, W. Sibbett, A. A. Zhilin, A. A. Lipovskii, "Nonlinear Spectroscopy of PbS Quantum-Dot-Doped Glasses as Saturable Absorbers for the Mode Locking of Solid-State Lasers," *J. Appl. Phys.*, **100** [2] 023108-5 (2006).

[3]V. G. Savitski, N. N. Posnov, P. V. Prokoshin, A. M. Malyarevich, K. V. Yumashev, M. I. Demchuk, A. A. Lipovskii, "Pbs-Doped Phosphate Glasses Saturable Absorbers for 1.3-μm Neodymium Lasers," *Appl. Phys. B: Lasers and Opt.*, **75** [8] 841-846 (2002).

[4]P. Bigenwald, V. V. Nikolaev, D. Solnyshkov, A. Kavokin, G. Malpuech, and B. Gil, "Polariton Lasers Based on Semiconductor Quantum Microspheres," *Phys. Rev. B*, **70** [20] 205343-6 (2004).

[5] S Cran-McGreehin, T. F. Krauss and K. Dholakia, "Integrated Monolithic Optical Manipulation," *Lab Chip*, **6** [9] 1122-1124 (2006).

[6]E. Palen, "Optical coupling to monolithic integrated photonic circuits," *Proc. of SPIE*, **6478**, 64780K-6 (2007).

[7]A. Lipovskii, E. Kolobkova, V. P. I. Kang, A. Olkhovets, T. Krauss, M. Thomas, J. Silcox, F. Wise Q. Shen and S. Kycia, "Synthesis and Characterization of Pbse Quantum Dots in Phosphate Glass," *Appl. Phys. Lett.*, **71** [23] 3406-3408 (1997).

[8]J. Chang, C. Liu and J. Heo, "Optical Properties of PbSe Quantum Dots Doped in Borosilicate Glass," *J. Non-Cryst. Solids*, **355** [37-42] 1897-1899 (2009).

[9]A. I. Filin, P. D. Persans, K. Babocsi, M. Schmitt, W. Kiefer, V. D. Kulakovskii and N. A. Gippius, "Effect of Nanocrystal Growth Conditions on Exciton Decay and Spin Dephasing in an Ensemble of Cdse Nanocrystals Grown in Glass," *Phys. Rev. B*, **73** [12] 125322-10 (2006).

[10]S. Joshi, S. Sen and P. C. Ocampo, "Nucleation and Growth Kinetics of PbS Quantum Dots in Oxide Glass: Spectroscopic and Microscopic Studies in the Dilute Range," *J. Phys. Chem. C*, **111** [11] 4105-4110 (2007).

[11]N. O. Dantas, R. S. Silva, and F. Qu, "Optical Properties of PbSe and PbS Quantum Dots Embedded in Oxide Glass," *Phys. Stat. Sol. (b)*, **232** [1] 177–181 (2002).

[12]H. Tichá, J. Schwarz, L. Tichý and R. Mertens, "Physical Properties of PbO-ZnO-P_2O_5 Glasses: II. Refractive Index and Optical Properties," *J. of Optoelect. and Adv. Mat.*, **6** [3] 747-753 (2004).

[13]J. Tauc, Amorphous and Liquid Semiconductor, Plenum Press, New York (1974).

[14]A. Paul, "Mechanism of Selenium Pink Colouration in Glass," *J. Mater. Sci.*, **10** [3] 415-421 (1975).

[15]L. S. Ramsdell, "The Crystal Structure of Some Metallic Sulfides," *American Mineralogist*, **10** [9] 281-304 (1925).

[16]Y. Masumoto and K. Sonobe, "Size-dependent Energy Levels of CdTe Quantum Dots," *Phys. Rev. B*, **56** [15] 9734-9737 (1997).

[17]I. Kang and F. W. Wise, "Electronic Structure and Optical Properties of PbS and PbSe Quantum Dots," *J. Opt. Soc. Am. B*, **14** [7] 1632-1646 (1997).

[18]J. A. Marqusee and J. Ross, "Kinetics of Phase Transitions: Theory of Ostwald Ripening," *J. Chem. Phys.*, **79** [1] 373-378 (1983).

[19]H. Yükselici, P. D. Persans and T. M. Hayes, "Optical Studies of the Growth of $Cd_{1-x}Zn_xS$ Nanocrystals in Borosilicate Glass," *Phys Rev. B*, **52** [16] 11763-11772 (1995).

[20]U. Morgner, F. Kärtner, S. Cho, Y. Chen, H. Haus, J. Fujimoto, E. Ippen, V. Scheuer, G. Angelow and T. Tschudi, "Sub-Two-Cycle Pulses from a Kerr-Lens Mode-Locked Ti:Sapphire Laser," *Opt. Lett.*, **24** [6] 411-413 (1999).

[21]M. Pollnau, C. Grivas, L. Laversenne, J. S. Wilkinson, R. W. Eason and D. P. Shepherd, "Ti:Sapphire Waveguide Lasers," *Laser Phys. Lett.*, **4** [8] 560-571 (2007).

[22]M. Haiml, R. Grange and U. Keller, "Optical Characterization of Semiconductor Saturable Absorbers," *Appl. Phys. B*, **79** [3] 331-339 (2004).

Figure Captions

Figure 1: (a) Shift in the band edge of the lead-phosphate glass with increase in PbSe mol%. (b) EDX spectrum of PZP10 glass. Inset shows the variation of weight percent of glass components with increase in PbSe mol%.

Figure 2: (a) Variation of refractive index of PZP0 and PZP10 glasses over the wavelength range 300 nm-1600 nm and (b) DTA curve of PZP10 glass.

Figure 3: (a) High resolution TEM image of PbSe QD-containing PZP glass heat treated at 380 ^{o}C for 12 hrs and (b) PbSe QD size distribution.

Figure 4: Magnified TEM image showing fringe patterns of PbSe QDs embedded in PZP glass (PZP10) heat treated at 380^{o}C for 12 hrs. Inset is the Fourier transform of d_{220} plane.

Figure 5: (a) Absorption spectra of bare glass (PZP0) (black solid line) and PbSe-containing (PZP10) glasses heat treated at 380 ^{o}C from 2 hrs to 24hrs, Inset: Variation of QD exciton peak with $1/t^{2/3}$ for longer dwelling times, dotted line is the linear fit (b) Plot of QD radius vs time, dotted lines are the fit at two regions (short and long dwelling times). Error bar shows a representative ± 0.2 nm variation in the measured QD radius and (c) Transmission vs. fluence at 1.2 μm for QD absorption peaked at 1.3 μm (indicated by * in (a)), solid line represents the least squares fit.

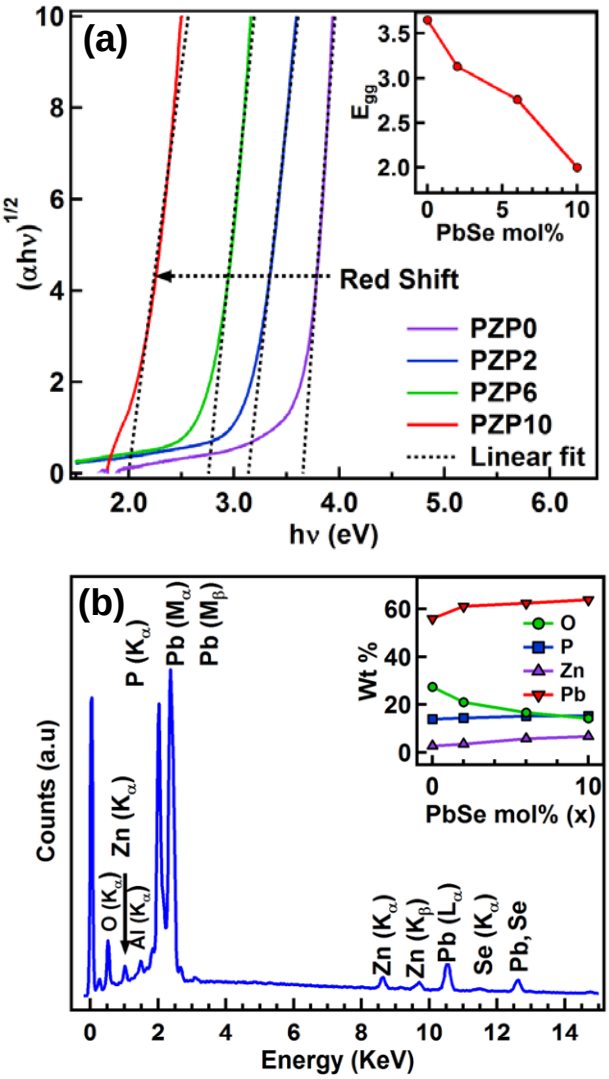

Fig.1: (a) Shift in the band edge of the lead-phosphate glass with increase in PbSe mol%. (b) EDX spectrum of PZP10 glass. Inset shows the variation of weight percent of glass components with increase in PbSe mol%.

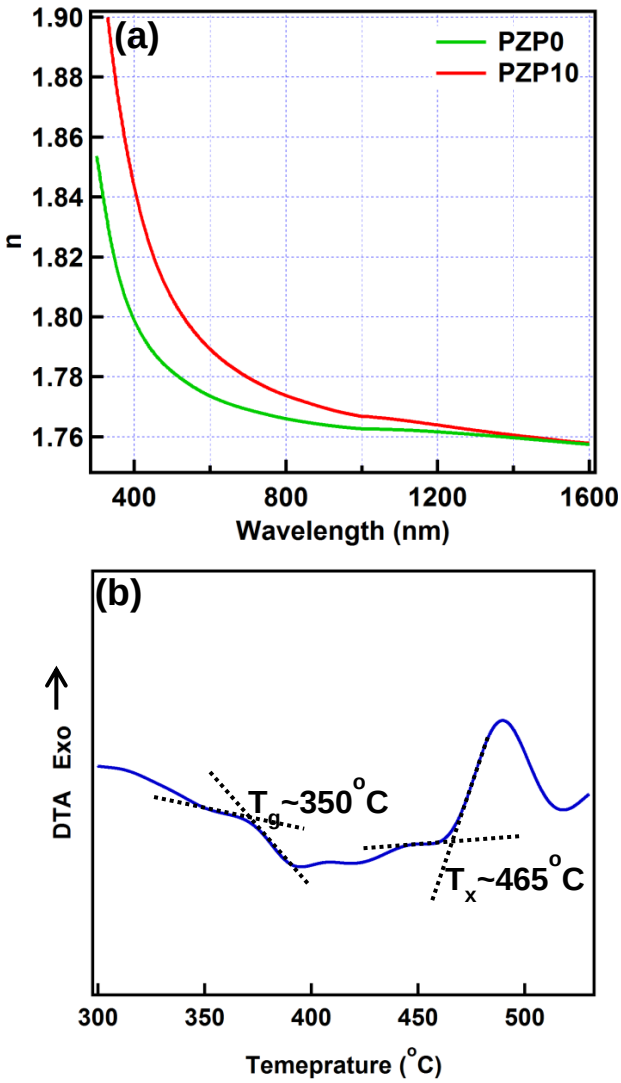

Fig. 2: (a) Variation of refractive index of PZP0 and PZP10 glasses over the wavelength range 300 nm-1600 nm and (b) DTA curve of PZP10 glass.

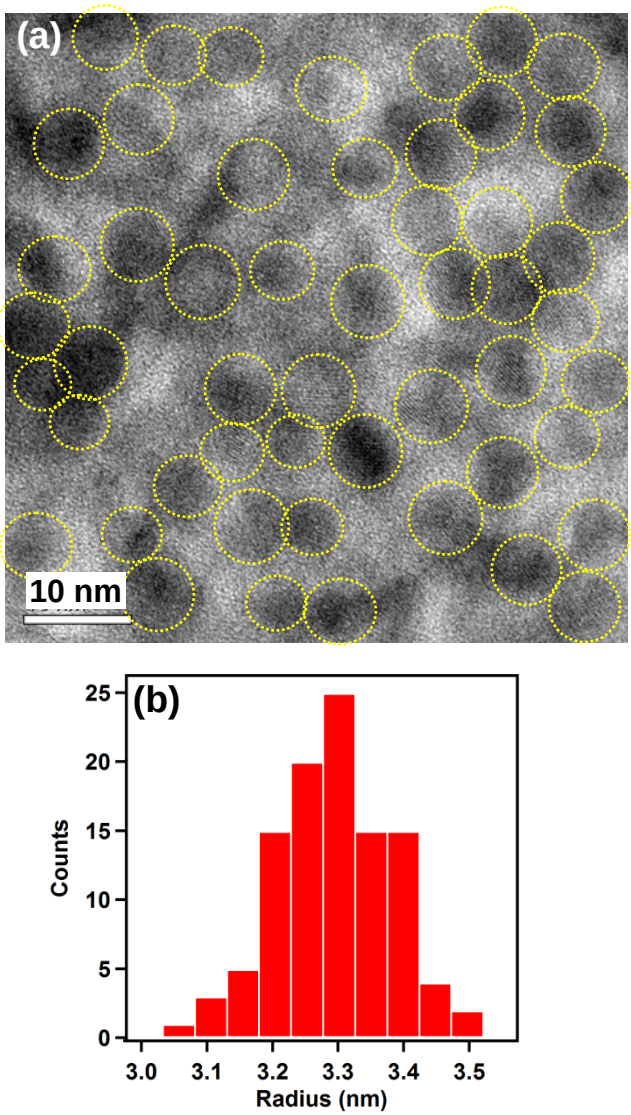

Fig. 3: (a) High resolution TEM image of PbSe QD-containing PZP glass heat treated at 380 ^{o}C for 12 hrs and (b) PbSe QD size distribution.

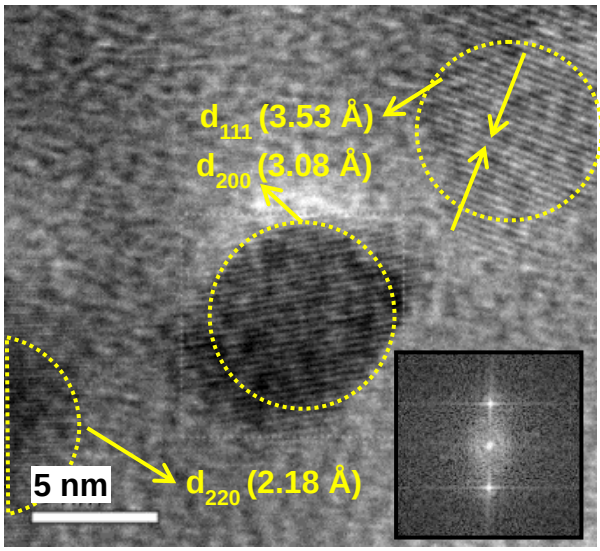

Fig. 4: Magnified TEM image showing fringe patterns of PbSe QDs embedded in PZP glass (PZP10) heat treated at 380°C for 12 hrs. Inset is the Fourier transform of d_{220} plane.

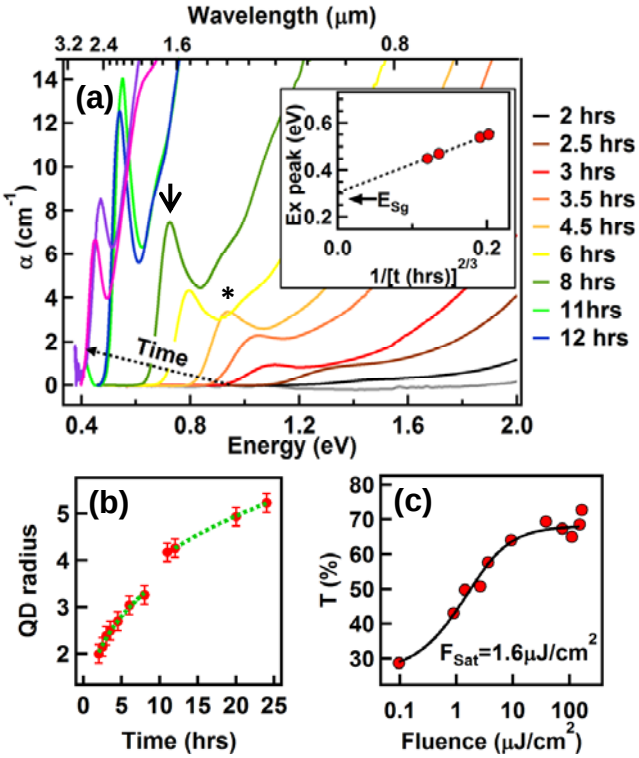

Fig. 5: (a) Absorption spectra of bare glass (PZP0) (black solid line) and PbSe-containing (PZP10) glasses heat treated at 380 ^{o}C from 2 hrs to 24hrs, Inset: Variation of QD exciton peak with $1/t^{2/3}$ for longer dwelling times, dotted line is the linear fit (b) Plot of QD radius vs time, dotted lines are the fit at two regions (short and long dwelling times). Error bar shows a representative ± 0.2 nm variation in the measured QD radius and (c) Transmission vs. fluence at 1.2 μm for QD absorption peaked at 1.3 μm (indicated by * in (a)), solid line represents the least squares fit.